

A NOVEL IMAGING TECHNIQUE FOR ANALYSIS OF ADJACENT SEGMENT KINEMATICS IN PATIENTS WITH ADULT IDIOPATHIC SCOLIOSIS

GANG LI, MD ^{a,b}; SHAOBAI WANG, BS ^{a,c}; MICHAL KOZANEK, MD ^a; PETER PASIAS, MD ^a; BRIAN GROTTKAU, MD ^a; GUOAN LI ^a, PHD; KIRKHAM B. WOOD, MD ^a

MASSACHUSETTS GENERAL HOSPITAL

INTRODUCTION

Adjacent segment degeneration following spine fusion remains a widely acknowledged problem, but there remains insufficient knowledge regarding the factors that contribute to its occurrence. Little is known about the kinematic characteristics of adjacent segments prior to surgical correction. We investigated the applicability of a novel imaging technique to measure the six degrees of freedom (6DOF) kinematics of adjacent segments prior to arthrodesis and instrumentation in a patient with idiopathic adult scoliosis,

METHODS

The kinematics of a 33 year old female with idiopathic scoliosis (major curve: T6-12, 55° by the Cobb method) with planned arthrodesis and instrumentation (T4-L2) were measured preoperatively in the adjacent segments (L2-L5) using a combined dual fluoroscopic imaging system (DFIS) and computer tomography (CT). We created three-dimensional (3D) models of the L2-L5 vertebrae from CT images using solid modeling software. Subsequently, the patient was fluoroscopically imaged at varied postures representing extremes of his spinal range of motion in 3 rotational planes: 1) maximal left/right twist, 2) left/right bending and 3) flexion/extension of the upper body. The vertebral models were then oriented used to match the fluoroscopic images to reproduce their in-vivo positions at each posture. The kinematics was then determined by

the relative positions and orientations of the proximal vertebra with respect to the distal vertebra.

RESULTS

The L2-3 motion segment had the greatest contribution to motion in the sagittal plane (11.9°) during flexion and extension of the spine (Table 1). The L4-5 motion segment was responsible for the majority of the rotation in the coronal plane during right and left bending (16.3°). Range of motion in the transverse plane during right and left twist of upper body was relatively small (less than 2° in each segment) and fairly equally distributed among the studied segments in the patient. We also observed that coupled translations in all primary rotations. Specifically, rotation in the sagittal plane was coupled with anterior-posterior translation whereas rotation in the coronal plane was coupled with translations in the left-right direction. These pilot data suggest that the motion of the patient with idiopathic adult scoliosis was not equally distributed among the vertebral segments.

CONCLUSION

This data was the first in vivo attempt at measuring kinematics in adult patients with scoliosis using DFIS and CT imaging technique. The data indicates that this technique is a potentially powerful tool that can effectively be applied to study the effects of surgery on the kinematics of adjacent vertebral motion segments in adult idiopathic scoliosis patients.

SIGNIFICANCE

Knowledge of kinematic changes before and after surgical correction in the vertebral segments adjacent to surgical arthrodesis is critical to understanding the mechanism of adjacent vertebral degeneration and may ultimately help improve the surgical treatment of adult idiopathic scoliosis and provide insight into the etiology of post-operative degeneration in adjacent segments. This novel DFIS and CT imaging technique has great potential in scoliosis research.

KEYWORDS

In-vivo scoliosis motion; vertebral kinematics; adjacent segment disease; spine biomechanics.

Introduction:

Spinal arthrodesis and instrumentation remains the standard surgical treatment for a variety of spinal deformities including adolescent idiopathic scoliosis, congenital scoliosis, adult scoliosis, kyphotic deformity and other specific spinal afflictions^{13,28}. Spinal arthrodesis and instrumentation alters the natural biomechanics of the spine and the absence of motion at the included segments is compensated by an increase at

^a Bioengineering Lab
Department of Orthopaedic Surgery
Massachusetts General Hospital/Harvard Medical School
Boston, MA

^b Department of Orthopaedic Surgery
Peking University Third Hospital/Peking University Health Science Center
Beijing, China

^c Department of Mechanical Engineering
Massachusetts Institute of Technology
Cambridge, MA

Corresponding address:

Guoan Li, PhD
Bioengineering Lab
Department of Orthopaedics
Massachusetts General Hospital
Harvard Medical School
55 Fruit Street, GRJ, 1215
Boston, MA 02114

gli1@partners.org

the adjacent unfused segments¹⁹. As a result, altered forces are transmitted across both the facet joints and inter-vertebral discs at the adjacent segments.¹⁴ These increased forces may thus lead to adjacent segment disease (ASD). The initial clinical improvement following a successful spinal arthrodesis has been shown to deteriorate over time as the segments adjacent to the fusion exhibit signs of accelerated disc degeneration, herniation of nucleus pulposus, spondylolysis, segment instability, spinal stenosis, and arthritis of the posterior facets.^{1,12,20,23,24,28}

Radiographic evidence of ASD has been reported to have a prevalence of more than 30%, and several perilous factors for its development have been suggested²⁸. These factors can be divided into two broad categories: patient factors and surgical factors. The most important patient factors include age,¹ obesity, preexisting degeneration of adjacent discs, menopause,⁶ and sacral inclination.¹² Proposed surgical factors have included length of arthrodesis, stiffness of the construct, aggressive decompression, disruption of facet capsules, loss of lumbar lordosis, and sagittal or coronal imbalance.²⁶

Despite their clinical importance, little is known about the kinematic characteristics of the vertebral segments adjacent to the instrumented levels of spines undergoing surgical correction for scoliosis mainly due to the technical challenge in measuring vertebral motion. In this study we focused on the region caudal to a planned scoliosis arthrodesis and instrumentation as it is here that ASD is most likely to occur. Our group has previously described normal spinal motion utilizing this technique.²⁷ In an effort to study ASD in an adult population undergoing surgery for deformity, we initially need to study the biomechanics of the untreated spine. A post-operative comparison with this data will be helpful not only in identifying the segments that may be at risk for ASD, but may also help future surgical technical planning and and implant design. We present a novel technique to quantitatively measure motion of the adjacent segments before surgical instrumentation and arthrodesis for adult scoliosis. The system has been previously used for the investigation of lumbar spine motion during weight bearing functional activities in normal individuals²⁷. In this study, we employed our DFIS/CT technique to determine the six degrees of freedom (6DOF) of vertebral motion in the lumbar spine (L2-L5) in various weight bearing positions of the upper body in a patient with adult idiopathic scoliosis slated to undergo surgical arthrodesis and instrumentation (T4-L2).

METHODS

PATIENT CHARACTERISTICS

The studied patient was a 33 year old woman with idiopathic scoliosis, recruited from the Massachusetts General Hospital Spine Center. Human Institutional Review Board approval for the study was obtained. The Cobb angle was measured as 55° (major right curve: T7-T11), the deformity was classified as Type 2 according to Lenke's classification and the lumbar spine modifier was determined as B¹⁵. The segments planned for surgical arthrodesis of instrumentation were T4 to L2 inclusive. The adjacent segments were considered to be L2-3

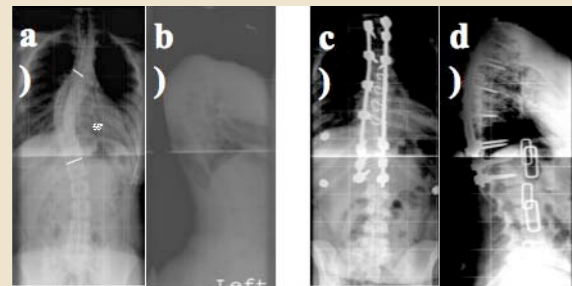
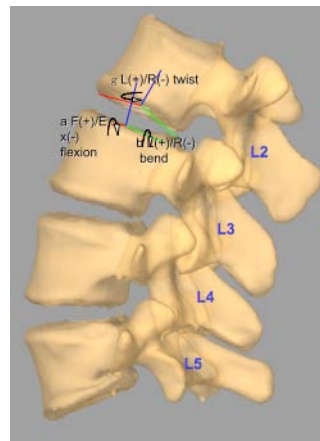


Fig 1. A female, 35, Idiopathic adult scoliosis (T6-T12). a) the preoperative AP shows 55° of Cobb angle; b) the preoperative film shows sagittal alignment; c) posterior instrumented spinal fusion from T2-L1, c) shows postoperative 2 weeks with Cobb 5° (T6-T12); d) shows the sagittal alignment of postoperative 2 weeks.



3D adjacent segment model of a scoliosis

Fig. 2: 3D anatomic adjacent segmental vertebral models from L2 to L5 constructed using the CT scans. Local coordinate systems at the endplates were used to calculate the relative 6DOF kinematics of the proximal vertebra with respect to distal vertebra.

L3-4 and L4-5 (Fig.1). We aimed to quantify the 6DOF kinematics of the adjacent segments during various weight bearing positions of the upper body.

THREE-DIMENSIONAL MODEL OF THE LUMBAR SPINE

First, parallel axial images of the lumbar spine were obtained using computer assisted tomography (CT) (GE Light Speed Pro 16-slice scanner) with a resolution of 512 x 512 pixels and a spacing of 1.5 mm. Each image was processed using a Canny edge filter programmed in a commercially available software package (Matlab, Mathworks, Canton, MA). The Canny filter calculates gradients in pixel intensity to detect edges between objects. The calculated edges were used to help trace the outlines of the vertebrae within each image using solid modeling software (Rhinoceros®, Robert McNeel & Associates, Seattle, WA). The contours were then placed in the appropriate plane in three-dimensional space and used to create a surface rendered mesh model¹⁶ (Fig. 2).

DUAL FLUOROSCOPIC IMAGING

Following CT scanning, the patient's lumbar spine was imaged using a dual fluoroscopic system. Two fluoroscopes (BV Pulsera, Phillips, Bothell, WA) were positioned with their image intensifiers perpendicular to each other in order to simultaneously capture images of the lumbar spine at different postures from two directions simultaneously (Fig. 2). The fluoroscope

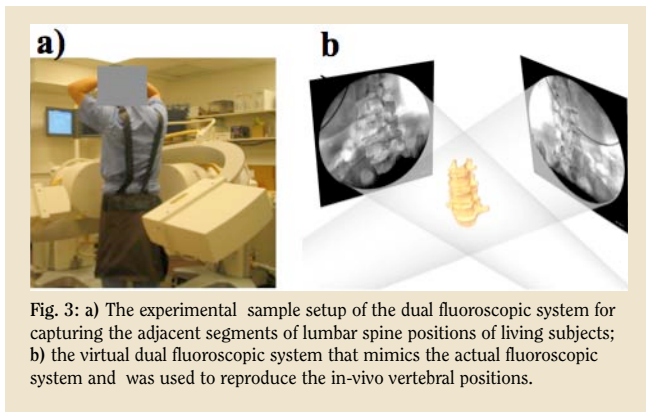


Fig. 3: a) The experimental sample setup of the dual fluoroscopic system for capturing the adjacent segments of lumbar spine positions of living subjects; b) the virtual dual fluoroscopic system that mimics the actual fluoroscopic system and was used to reproduce the in-vivo vertebral positions.

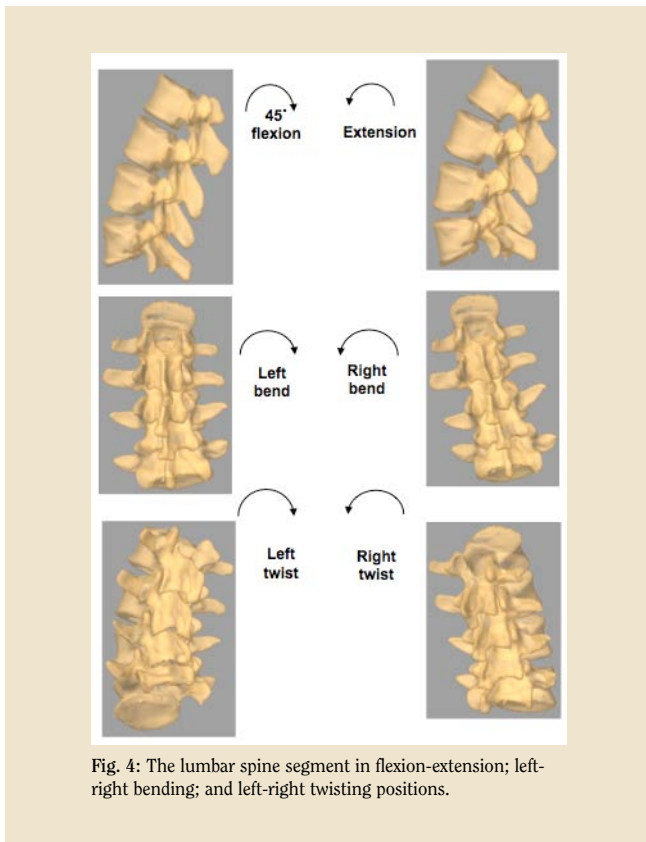


Fig. 4: The lumbar spine segment in flexion-extension; left-right bending; and left-right twisting positions.

has a clearance of approximately 1 m between the X-ray source and the receiver, allowing the subject to be imaged by the fluoroscopes simultaneously while performing different maneuvers. The total imaging volume can reach up to 30x30x30 cm³.

Initially, the subject was asked to stand upright with the lumbar spine positioned within the field of view of both fluoroscopes. Next, the patient was asked to actively move to varied postures in a predetermined sequence: standing position; 45° flexion; maximal extension; maximal left-right bending; maximal left-right twisting. The two laser guides attached to the fluoroscopes aided in positioning the patient's lumbar spine within the field of view of the two fluoroscopes.

IN-VIVO SPINE KINEMATICS

Pairs of fluoroscopic images captured at specific postures were imported into the modeling software and placed in calibrated orthogonal planes, reproducing the actual positions of the image intensifiers. Two virtual cameras were created inside the animated space to reproduce the positions of the x-ray sources with respect to the image intensifiers. Thereby, the geometry of the dual-orthogonal fluoroscopic system was recreated in the solid modeling program. The CT image-based 3D vertebral models were introduced into the virtual fluoroscopic system and viewed from the perspective of the two virtual cameras (Fig. 3). The 3D models of the vertebrae could be independently moved and rotated in space until In this manner, the position of each vertebra during the studied weight-bearing activities could be reproduced (Fig. 4).

After reproducing the in-vivo vertebral positions, the relative motion of the vertebrae were analyzed using right handed Cartesian coordinate systems constructed at the endplates of each vertebra (Fig. 2). The geometric center of the endplate was chosen as the origin of the coordinate system²⁷. The X-axis was in the frontal plane and pointed to the left direction; the Y-axis was in sagittal plane and pointed to the posterior direction; and the Z-axis was vertical to the X-Y plane and pointed proximally.

At each segment, the relative motion of the cephalad vertebra with respect to the caudal vertebra was calculated for 3 vertebral levels: L2-3, L3-4 and L4-5. Three translations were defined as the motions of the origin of the cephalad vertebral coordinate system in the caudal coordinate system: anterior-posterior, left-right and distal-proximal translations. Three rotations were defined as the orientations of the cephalad vertebral coordinate system in the caudal vertebral coordinate system using Euler angles (in X-Y-Z sequence): flexion-extension left-right bending and left-right twisting rotations (Fig. 2).

After determining the vertebral positions at each posture, we measured the range of motion of each vertebral level between the studied postures of flexion-extension, left-right bending and left-right twisting²⁷. The range of motion data included both the primary rotations and coupled translations and rotations in the other 5 degrees of freedom.

RESULTS

PRIMARY MOTIONS

During forward and backward bending of upper body, the L2-3 level had the greatest contribution to the motion of the lumbar spine in the sagittal plane (11.9°). During left-right bending, the upper levels had smaller contributions to the motion in the coronal plane than the lower levels (Table. 1). Specifically, the L4-5 had a 16.3° range of coronal rotation during side-to-side bending, which was more than ten-times larger than at either the L2-3 or the L3-4 level. For the left-right twist, the three vertebral levels demonstrated similar ranges in the transverse-plane rotation. (Table.1). The greatest and smallest transverse-plane rotations were 2.0° at L2-3 and 0.4° for L3-4 levels, respectively.

Motion	Segment	Translation			Rotational plane		
		L/R [mm]	A/P [mm]	S/I [mm]	Sagittal [°]	Coronal [°]	Transverse [°]
Left/Right Twist	L2 - L3	1.0	0.6	0.2	1.7	1.9	2.0
	L3 - L4	0.0	0.7	0.9	1.3	2.4	0.4
	L4 - L5	0.7	1.2	0.0	1.1	1.0	1.7
Left/Right Bending	L2 - L3	0.3	1.2	0.3	2.8	1.5	0.0
	L3 - L4	1.8	1.9	0.8	1.0	1.4	0.2
	L4 - L5	7.2	0.2	0.8	0.5	16.3	1.4
Flexion/Extension	L2 - L3	1.1	4.2	1.8	11.9	2.1	0.9
	L3 - L4	0.1	0.8	0.6	2.3	0.8	3.2
	L4 - L5	3.0	0.8	2.2	5.0	6.2	1.5

Table 1. Kinematics of the adjacent vertebral segments in the patient with adult idiopathic scoliosis during the 3 weight-bearing activities: flexion-extension, left-right bending and left-right twisting. The coupled translations are labeled as LR (left-right translation), AP (anterior-posterior translation) and SI (superior-inferior translation). The ranges of the 3 rotations were labeled as FE (flexion extension), Bend (left-right bending) and Twist (left-right twisting).

COUPLED TRANSLATIONS AND ROTATIONS

During the active flexion-extension motion, we observed coupled translations in all three directions of the coordinate system (Table 1). For example, in the L2-3 segment, the range of translation of L2 relative to L3 was 1.1 mm in the left-to-right direction, 1.8 mm in the superior-inferior direction and 4.2 mm in the anterior-posterior direction. During the active left-right bending motion, the greatest translational motion was observed in the L4-5 segment in left-to-right direction (7.2 mm). The coupled translations in the remaining directions were all less than 2.0 mm. During the left-right twisting motion of upper body, the translations in all directions are relatively small. For instance, mean translation was 0.37 mm in the superior-inferior direction at L2-5.

DISCUSSION

In this study, we investigated the feasibility of a combined dual fluoroscopy and CT imaging technique of measuring the kinematics of vertebral segments distal to levels for planned surgical arthrodesis and instrumentation (L2-5). This was undertaken in a patient with adult idiopathic scoliosis with a right-sided thoracic curve who was scheduled for surgical correction. The study demonstrated that the more rostral segments (L2-3) had the greatest contribution to motion in the sagittal plane whereas the more caudal segments (L4-5) had a greatest contribution to motion in the coronal plane. Motion in the transverse plane was fairly equally distributed across the studied vertebral motion segments of the lumbar spine (L2-5) during all studied activities. We also observed that translational motion is coupled with spinal rotation. Specifically, rotation in the sagittal plane was coupled with anterior-posterior translation whereas rotation in the coronal plane was coupled with translations in left-right direction.

Quantitative data on *in-vivo* vertebral motion is critical to the understanding of segmental spinal degeneration and in uncovering factors involved in its genesis in spinal deformity.

However, it has been a challenge to quantitatively describe vertebral motion *in vivo*. No previous study investigated the *in-vivo* motion of vertebral segments during unrestricted functional activities in adult idiopathic scoliosis. Several radiographic studies have reported on normal spinal motion. Percy et al.²² investigated lumbar spinal motion using a form of stereo-radiography in normal individuals, however, the pelvis and hips were limited in motion by using a rig. Haughton et al.⁹ and Ochia et al.²¹ studied passive axial rotation of the body in supine position using magnetic resonance and CT reconstruction, respectively. Haughton et al. rotated the subject's hip $\pm 8^\circ$ to investigate the lumbar spine rotation that provided separate supports for the torso, hips and legs, while Ochia et al. rotated the upper body $\pm 50^\circ$ to measure the lumbar spine rotation. In both of these *in-vivo* studies, however, the spine was not under functional weight bearing conditions. Lim et al.¹⁷ also used CT scan of two cervical vertebrae to verify an Eigen vector method and revealed that method had an accuracy of 1mm in translation and 1° in rotation. The accuracy and reproducibility of similar imaging methods have been validated by others using phantoms composed of ceramic balls^{11,21}. While using the combined DFIS and CT imaging technique, a similar phantom study using various beads has been conducted to validate the its accuracy of the dual fluoroscopic imaging method used in this study and reported an accuracy of less than 0.08 mm in translation and 0.2° in rotation.² In this study, we demonstrated that the DFIS and CT imaging technique can be used to study symptomatic scoliosis patients during maximal left-right bending and left-right twisting of the upper body in the upright position.

Studies of the adjacent segment pathology in the literature focus primarily on the clinical outcomes or compare fusion with non-fusion outcomes at follow-up.^{3-5,8,10,18,25} Yang et al.²⁸ reported the impact of ASD on the clinical outcome after lumbar spinal fusion showing significant correlation, especially

with multiple-segment fusion. Cho et al,⁵ compared the ASD developed results between short fusion and long fusion for degenerative lumbar scoliosis. They found long fusion should be carried out to minimize ASD at follow up. None of these studies investigated the pathology of ASD. Using the combined DFIS and CT imaging technique, we will be able to detect the vertebral motion adjacent to the involved segment preoperatively, thus, we may be able to examine the effect of distal vertebral motion on the ASD.

There are several limitations to the current study. In order to maintain the targeted adjacent segments of the lumbar spine within the field view of the two fluoroscopes, the subject was instructed to limit flexion to approximately 45° from a standing position. Also, we examined the range of motion of the L2-3, L3-4 and L4-5 segments during 3 functional motions of the upper body in one scoliosis subject preoperatively. We did not examine the *in-vivo* instantaneous positions of the adjacent segments of lumbar spine during dynamic motion of the body. However, this pilot study demonstrated the feasibility of combined CT and dual fluoroscopy of measuring *in vivo* spine kinematics in spinal deformity. We plan on studying adult idiopathic scoliosis patients pre- and post-operatively to quantify the biomechanical changes occurring in the vertebral segments adjacent to the arthrodesis and instrumentation.

In conclusion, this study utilized a simultaneous dual-fluoroscopic system to measure the kinematics of the segments adjacent to a planned surgical correction pre-operatively in a patient with thoracic scoliosis under weight bearing conditions. The results showed that the cephalad level (L2-3) in this particular patient had greatest contribution to the motion in the sagittal plane by coupling flexion-extension rotation and anterior-posterior translation. Additionally, the caudal level (L4-5) contributed most to the motion in the coronal plane by coupling left-right rotation and left-right translation. The advantage of this system for spinal research is its flexibility to accommodate various functional activities. This technique will provide a powerful tool for investigation of the *in-vivo* function of the spine in spinal deformity. Future investigations will be directed at comparing the kinematic differences of adjacent segments before and after surgical treatment for scoliosis as well as others with different forms of spinal deformity.

ACKNOWLEDGEMENT

This study was funded through a NASS research grant and by the Department of Orthopaedic Surgery at the Massachusetts General Hospital. The authors would like to thank Lisa Beyer C., PA for her testing communication assistance.

References

1. Aota, Y.; Kumano, K.; and Hirabayashi, S.: Postfusion instability at the adjacent segments after rigid pedicle screw fixation for degenerative lumbar spinal disorders. *J Spinal Disord*, 8(6): 464-73, 1995.
2. Bingham, J., and Li, G.: An optimized image matching method for determining in-vivo TKA kinematics with a dual-orthogonal fluoroscopic imaging system. *J Biomech Eng*, 128(4): 588-95, 2006.
3. Cheh, G.; Bridwell, K. H.; Lenke, L. G.; Buchowski, J. M.; Daubs, M. D.; Kim, Y.; and Baldus, C.: Adjacent segment disease following lumbar/thoracolumbar fusion with pedicle screw instrumentation: a minimum 5-year follow-up. *Spine*, 32(20): 2253-7, 2007.
4. Cho, K. J.; Suk, S. I.; Park, S. R.; Kim, J. H.; Kim, S. S.; Choi, W. K.; Lee, K. Y.; and Lee, S. R.: Complications in posterior fusion and instrumentation for degenerative lumbar scoliosis. *Spine*, 32(20): 2232-7, 2007.
5. Cho, K. J.; Suk, S. I.; Park, S. R.; Kim, J. H.; Kim, S. S.; Lee, T. J.; Md; Lee, J. J.; and Lee, J. M.: Short fusion versus long fusion for degenerative lumbar scoliosis. *Eur Spine J*, 2008.
6. Etebar, S., and Cahill, D. W.: Risk factors for adjacent-segment failure following lumbar fixation with rigid instrumentation for degenerative instability. *J Neurosurg*, 90(2 Suppl): 163-9, 1999.
7. Goel, V. K.; Clark, C. R.; McGowan, D.; and Goyal, S.: An in-vitro study of the kinematics of the normal, injured and stabilized cervical spine. *J Biomech*, 17(5): 363-76, 1984.
8. Good, C.: Re: Kolstad F, Nygaard OP, Leivseth G. Segmental motion adjacent to anterior cervical arthrodesis: a prospective study. *Spine* 2007;32:512-7. *Spine*, 32(18): 2035-6, 2007.
9. Houghton, V. M.; Rogers, B.; Meyerand, M. E.; and Resnick, D. K.: Measuring the axial rotation of lumbar vertebrae in vivo with MR imaging. *AJNR Am J Neuroradiol*, 23(7): 1110-6, 2002.
10. Hwang, S. H.; Kayanja, M.; Milks, R. A.; and Benzel, E. C.: Biomechanical comparison of adjacent segmental motion after ventral cervical fixation with varying angles of lordosis. *Spine J*, 7(2): 216-21, 2007.
11. Ishii, T.; Mukai, Y.; Hosono, N.; Sakaura, H.; Nakajima, Y.; Sato, Y.; Sugamoto, K.; and Yoshikawa, H.: Kinematics of the upper cervical spine in rotation: in vivo three-dimensional analysis. *Spine*, 29(7): E139-44, 2004.
12. Kumar, M. N.; Baklanov, A.; and Chopin, D.: Correlation between sagittal plane changes and adjacent segment degeneration following lumbar spine fusion. *Eur Spine J*, 10(4): 314-9, 2001.

13. **Kumar, M. N.; Jacquot, F.; and Hall, H.:** Long-term follow-up of functional outcomes and radiographic changes at adjacent levels following lumbar spine fusion for degenerative disc disease. *Eur Spine J*, 10(4): 309-13, 2001.
14. **Lee, C. K., and Langrana, N. A.:** Lumbosacral spinal fusion. A biomechanical study. *Spine*, 9(6): 574-81, 1984.
15. **Lenke, L. G.; Betz, R. R.; Harms, J.; Bridwell, K. H.; Clements, D. H.; Lowe, T. G.; and Blanke, K.:** Adolescent idiopathic scoliosis: a new classification to determine extent of spinal arthrodesis. *J Bone Joint Surg Am*, 83-A(8): 1169-81, 2001.
16. **Li, G.; DeFrate, L. E.; Park, S. E.; Gill, T. J.; and Rubash, H. E.:** In vivo articular cartilage contact kinematics of the knee: an investigation using dual-orthogonal fluoroscopy and magnetic resonance image-based computer models. *Am J Sports Med*, 33(1): 102-7, 2005.
17. **Lim, T. H.; Eck, J. C.; An, H. S.; McGrady, L. M.; Harris, G. F.; and Haughton, V. M.:** A noninvasive, three-dimensional spinal motion analysis method. *Spine*, 22(17): 1996-2000, 1997.
18. **Liu, F.; Cheng, J.; Komistek, R. D.; Mahfouz, M. R.; and Sharma, A.:** In vivo evaluation of dynamic characteristics of the normal, fused, and disc replacement cervical spines. *Spine*, 32(23): 2578-84, 2007.
19. **McAfee, P. C.; Cunningham, B. W.; Hayes, V.; Sidiqi, F.; Dabbah, M.; Seftor, J. C.; Hu, N.; and Beatson, H.:** Biomechanical analysis of rotational motions after disc arthroplasty: implications for patients with adult deformities. *Spine*, 31(19 Suppl): S152-60, 2006.
20. **Nagata, H.; Schendel, M. J.; Transfeldt, E. E.; and Lewis, J. L.:** The effects of immobilization of long segments of the spine on the adjacent and distal facet force and lumbosacral motion. *Spine*, 18(16): 2471-9, 1993.
21. **Ochia, R. S.; Inoue, N.; Renner, S. M.; Lorenz, E. P.; Lim, T. H.; Andersson, G. B.; and An, H. S.:** Three-dimensional in vivo measurement of lumbar spine segmental motion. *Spine*, 31(18): 2073-8, 2006.
22. **Pearcy, M. J.:** Stereo radiography of lumbar spine motion. *Acta Orthop Scand Suppl*, 212: 1-45, 1985.
23. **Penta, M.; Sandhu, A.; and Fraser, R. D.:** Magnetic resonance imaging assessment of disc degeneration 10 years after anterior lumbar interbody fusion. *Spine*, 20(6): 743-7, 1995.
24. **Rahm, M. D., and Hall, B. B.:** Adjacent-segment degeneration after lumbar fusion with instrumentation: a retrospective study. *J Spinal Disord*, 9(5): 392-400, 1996.
25. **Robertson, P. A. Re: Kolstad F, Nygaard OP, Leivseth G. Segmental motion adjacent to anterior cervical arthrodesis: a prospective study. Spine 2007;32:512-7. Spine**, 32(18): 2035, 2007.
26. **Schlegel, J. D.; Smith, J. A.; and Schleusener, R. L.:** Lumbar motion segment pathology adjacent to thoracolumbar, lumbar, and lumbosacral fusions. *Spine*, 21(8): 970-81, 1996.
27. **Wang S, L. G., Passias P, Li Guoan, Wood Kirk. :** Measurement of Vertebral Kinematics Using Non-invasive Image Matching Method - Validation and Application. *Spine*, 2008.
28. **Yang, J. Y.; Lee, J. K.; and Song, H. S.:** The impact of adjacent segment degeneration on the clinical outcome after lumbar spinal fusion. *Spine*, 33(5): 503-7, 2008.